

Development and Fabrication of Capacitive Sensors in Polyimide

Michael Pedersen, Wouter Olthuis and Piet Bergveld

MESA Research Institute, University of Twente, P.O. Box 217,
NL-7500 AE Enschede, the Netherlands

(Received February 21, 1997; accepted July 23, 1997)

Key words: silicon sensors, integrated sensors, capacitive sensors, polymer processing, polyimide

This paper deals with the development and implementation of polyimide technology in micromechanical capacitive sensors. The paper includes a review of polyimide technology in MEMS and IC processes, from which a low-temperature ($< 300^{\circ}\text{C}$) modular sensor process has been developed, whereby sensors can be fabricated directly on substrates containing complete electronic circuits. The capacitive sensors implemented include a condenser microphone, a pressure sensor, and a uniaxial accelerometer. The results from measurements on these sensors indicate that IC-compatible sensors exhibiting good performance can be achieved with the polyimide technology, and it is suggested that the use of polymer processing on silicon, therefore, may become an important aspect of smart sensors of the future.

1. Introduction

The development of smart systems and systems with adaptive properties is largely a problem associated with control engineering. However, in order to derive a precise and sufficient control strategy, detailed knowledge about the properties and conditions within the system must be determined. The sensor is therefore essential as it provides the information necessary to control the system. As a higher degree of precision and controllability of the system is required, so must the sensors provide this type of information. In most cases this leads to the conclusion that a higher distribution of sensors is necessary to provide adequate information.

In some cases, a higher distribution of conventional sensors is not feasible due to limitations of weight, size, and price. With the introduction of sensors made by silicon micromachining,⁽¹⁾ new possibilities for the miniaturization of the measurement systems have emerged. The potential integration of sensors and signal detection circuits on the same silicon chip yields not only the greatest possible miniaturization, but also a higher flexibility and simplification of the structure of the complete system, i.e., if a standard system (a bus) is used between the sensors and the rest of the system. Such integrated sensors, known as smart sensors,⁽²⁾ are devices which not only detect a certain physical quantity, but also have the onboard capabilities to transform the signal into a standard form, thereby allowing a standard interface with the control system. This modular approach is of great value in any system, and the tiny integrated silicon sensors can provide new applications in systems with small dimensions, which had previously been difficult to control. Furthermore, the integrated silicon sensors have proven to be applicable in systems where size is not absolutely critical (*e.g.*, airbag systems in cars),⁽³⁾ which is mainly due to the fabrication potential of very large numbers of devices at a relatively low price associated with the silicon technology. Additionally, there are sensing principles through which performance/precision can be directly improved by integrating a signal detection circuit in close proximity. This is especially true for capacitive sensors where the parasitic capacitance of the interconnection between the sensor and the detection circuit can greatly influence the performance; this is normally the problem that obstructs the use of the otherwise superior capacitive sensors regarding sensitivity and power consumption.

Bringing together the very strict IC technology and the more open MEMS technology poses significant problems, especially since one wants to preserve the control of the very complex IC technology. This desire leads to the conclusion that if any sensor is to be made on a chip that also contains integrated circuits, it must be carried out in a manner which will not in any way influence the performance of the integrated circuits. This means that in no way should the IC process be interfered with or interrupted, as this is certain to influence the device characteristics. Consequently, the sensor must be fabricated either by the IC process itself, or by a process that can be performed without affecting the integrity of the IC process. The delicacy of the IC technology, however, leaves very few MEMS fabrication processes which are directly compatible. First, the process temperature should be kept under 350–400°C to ensure the stability of the aluminium interconnection layers and to avoid exceeding the limit of mechanical stress which could cause damage, *e.g.*, cracks, in the IC structures. Second, a number of low-temperature processes are known to influence IC devices, including e-beam evaporation,⁽⁴⁾ plasma-enhanced chemical vapor deposition (PECVD), and RF sputtering.⁽⁵⁾ Lastly, the etching of silicon with liquid chemicals, such as potassium hydroxide (KOH), requires that the IC structures be physically protected from the liquid, as it will instantly destroy the structure. Achieving this protection on 4", 6", or 8" substrates may prove very difficult, and wet chemical etching of silicon should therefore be avoided.

In this paper we describe how the introduction of polyimide processing can make the sensor process fully compatible with IC structures. The description of the MEMS sensor process based on polyimide will be preceded by a brief review and an investigation of the processing and most important properties of polyimide, which affect the performance of

the sensor. Furthermore it will be shown that the modular sensor process can be applied to the fabrication of numerous types of capacitive sensors, requiring only a modification of the photolithographic masks in the process, thereby also allowing the fabrication of different sensors on the same silicon substrate.

2. Polyimide Technology Applied in Silicon Micromachining

Polymers comprise a group of materials that remain to be exploited in micromachining technology. The major reasons for this are the well-known problematic properties of most polymers, such as water absorption, chemical and thermal instabilities, and viscoelastic properties. However, from the processing point of view, these materials are ideally suited for sensor processes to be integrated with IC processes, since the application and definition of such layers is very simple, and can normally be done with the same spin-on technology used for photoresist layers in lithographic processes. Considering the restrictions mentioned above, it is an interesting prospect to consider the use of polymers in an IC-compatible sensor process. However, a polymer that has good chemical and mechanical properties that can withstand the other processing steps still required to create the complete sensor must be used. Polyimide is considered a suitable polymer for this purpose, and it is a material which has already been investigated extensively and has been used as a passivation and insulation layer in IC technology. In the following, the most important properties of micromechanical parts of sensors made of this material will be discussed.

2.1 *Polyimide chemistry and processing*

Polyimide compounds are classified as cyclic-chain polymers. They are characterized by the presence of an imide functionality, i.e., a cyclic amine bound to two of the carbonyl groups, surrounding the aliphatic or aromatic group in the main chain.

The basic procedure for the synthesis of polyimide is initiated by first forming a polyamic acid by a polycondensation reaction of an acid dianhydride and a difunctional base (diamine). The polyamic acid precursor formed by this reaction is soluble in polar inorganic solvents, such as *n*-methylpyrrolidone (NMP), dimethyl formamide (DMF) and dimethylsulfoxide (DMSO). The polyamic acid can subsequently be imidized by applying energy (heat), whereby the solvent is removed and a chemical reaction (ring closure) is induced. During the ring closure, water is expelled from the molecular structure in an irreversible reaction, thereby forming the polyimide. This heat treatment, known as "curing", is typically carried out at a temperature ranging from 300°C to 500°C. The temperature required to imidize the polymer depends on the exact materials used for the synthesis. Since, the imidization is irreversible the polyimide cannot, in principle, absorb water; however, since these kinds of processes are statistical, perfect imidization can never be obtained, wherefore sites always remain in the polymer chains where water molecules may be bound. The completeness of imidization and the cross-linking formed has a direct influence on the polyimide properties, such as thermal, mechanical and electrical stability. For the commercialization of these materials, numerous types of polyamic acids have been developed, however, the most common and well-documented synthesis is based on

pyromellitic acid dianhydride (PMDA) and oxydianiline (ODA), which form a polyimide known as the duPont® Kapton® film⁽⁶⁾ that is widely used in packaging processes. The processing of polyimide in microtechnology makes use of the already well-known spin-on technology used for fabricating resists in photolithography. Typically, the resins used to form the polyimide films are solutions containing the polyamic acid precursor dissolved in one of the organic solvents mentioned above. Such polyimide resins based on different syntheses are commercially available from different suppliers, including duPont® (PI), Hitachi (PIQ) and Ciba-Geigy (Probimide™).

In principle, two methods to pattern the polyimide layer exist,⁽⁷⁾ as shown in Fig. 1. After spinning on the precursor and removing the solvent by prebaking, the film can be immediately cured. However, after curing, the polyimide film becomes insoluble in virtually all chemicals. Only hot bases and very strong acids will dissolve the material. Since masking against such chemicals is very difficult, dry etching by means of an oxygen plasma is normally applied. For this purpose, a metal mask must be deposited and patterned on top of the polyimide, and then removed. A simpler method, shown in Fig. 1(b), is not to cure the precursor directly after spinning, but instead to apply a photoresist layer on top. Since the precursor is dissolved in the basic photoresist developer, the pattern in the resist will be transferred directly to the polyimide during development of the photoresist. The photoresist may subsequently be stripped, using a chemical that does not dissolve the precursor (*e.g.*, acetone), and the polyimide pattern can then be formed by curing. Wet chemical etching is attractive because of its simplicity; however, since patterning with the photoresist developer is difficult to control, the dry etching method offers higher resolution (typically 5 times), which is why this method is preferred in IC technology. Good adhesion of the polyimide film on the underlying substrate is critical for the stability of the component containing the film, and has been investigated extensively.⁽⁷⁾
⁻¹⁰⁾ It has been found that the adhesion on normally hydrolyzed surfaces may be signifi-

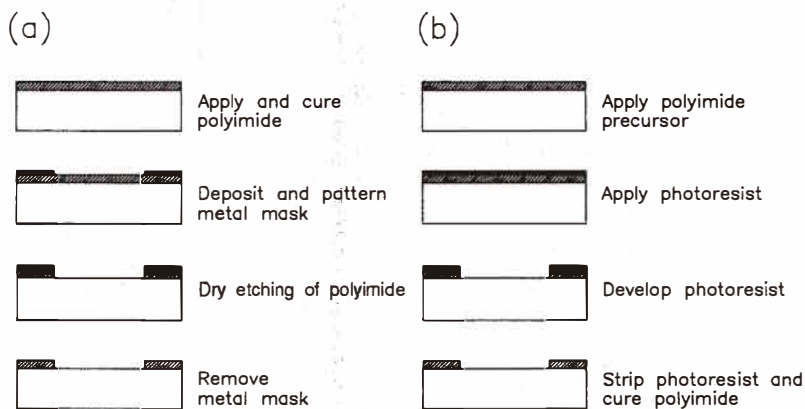


Fig. 1. Processing of polyimide. (a) Patterning by dry etching. (b) Patterning by photolithography.

cantly improved by applying a silane-based promoting agent to the substrate immediately before spinning the polyimide precursor. This surface treatment will improve the adhesion on surfaces such as silicon and the derivatives (oxide, nitride, oxynitride) of aluminium and copper. However, adhesion still deteriorates over time. One of the few materials in which no deterioration of adhesion has been detected is chromium.⁽⁸⁻¹⁰⁾ Furthermore, experiments have shown that no adhesion promotion is required on chromium surfaces.⁽⁹⁾

Another important polyimide technology that has emerged is the application of photosensitive polyimides.^(7,11) The precursor for this type of polyimide is derived in the same manner as described above, and is typically based on PMDA-ODA synthesis. However, the carboxylic groups in the polyamic acid have been esterified with photoreactive acrylic-methacrylic groups. Upon illumination, these groups react, forming cross-links of the polyamic acid, causing it to become insoluble. This way, the polyimide precursor acquires the properties of a negative photoresist and may be processed using conventional lithography, and then developed using one of the organic solvents mentioned above. During the imidization of the polyimide precursor, the cross-linked photosensitive groups are depolymerized and expelled from the polymer. Compared to conventional polyimides, this additional cleavage causes the film to shrink further during imidization, and therefore the resolution of photosensitive polyimides is inferior to that of polyimides. Considering, however, the processing of photosensitive polyimide, it is clear that the fabrication of these layers is much simpler than the processes shown in Fig. 1. Commercial resins of photosensitive polyimide are available from a number of suppliers, such as OCG Microelectronics HTR 3 series, duPont® E38675-50, Ciba-Geigy Probimide™ 300 series, and Hitachi PL-1100.

2.2 Polyimide properties

As mentioned above, polyimide is currently being used for passivation and insulation layers in IC technology and hybrid packaging. Therefore, comprehensive research into the electrical and mechanical properties of polyimide films has been conducted.

2.2.1 Electrical properties

The electrical properties of polyimide are essential in IC technology, since they directly influence the performance of the circuit. The issues investigated include the dielectric constant, dielectric loss, and electrical breakdown and leakage. From these investigations a relative dielectric constant of 3.1–3.5 for PMDA-ODA polyimide has been reported. However, this value depends on the film thickness,⁽¹²⁾ temperature⁽¹²⁾ and relative humidity.⁽⁹⁾ An increase in any of these parameters will cause the dielectric constant to increase. Most significantly, changes of up to 35% of the dielectric constant over the full relative humidity range have been reported.⁽⁹⁾ For this reason, polyimide is also suited for use in humidity sensors. This dependence on humidity is explained by the adsorption of water molecules in the free space within the polymer. Since the relative dielectric constant of water is high ($\epsilon_r \approx 80$), small amounts of water will influence the dielectric constant. Measurements have shown that a PMDA-ODA polyimide film will absorb between 2.5% and 3.5% of its own weight in water. The dissipation factor $\tan \delta$, which accounts for the dielectric loss in the film, has been found to be 0.7×10^{-3} to 3×10^{-3} for the full relative

humidity range,⁽⁹⁾ and was found to be a function of the curing temperature of the polyimide.⁽¹³⁾ It has been shown that a minimum dissipation factor occurs when the film is fully cured.⁽¹³⁾ Further experiments show that the dissipation is also smaller if the polyimide is cured in nitrogen instead of air.⁽¹³⁾ The breakdown electrical field has been measured to be between 3.3 MV/cm and 1.6 MV/cm for relative humidities between 0% and 100%,⁽⁹⁾ and the resistivity was found to depend on the curing conditions, film thickness, temperature and field strength.⁽¹²⁾ Typical resistivities measured at room temperature are in the range of $10^{16} \Omega\text{cm}$.⁽¹²⁾

2.2.2 Mechanical properties

In IC technology, the mechanical properties of the polyimide affect the stability of the component, not the performance directly. However, if the material is to be used in a mechanical sensor, these properties will determine the performance of the sensor and therefore must be known. Several researchers have studied this;^(9,14,15) however, since these parameters depend on the exact polyimide resin and the preparation conditions of the film, more experiments are needed to determine the actual properties.

The intrinsic stress in the polyimide film is generated due to the mismatch of the coefficient of thermal expansion (CTE) between the film and the substrate. Since the CTE of polyimide can be as high as 50 ppm/°C,⁽¹⁴⁾ compared to 3 ppm/°C for silicon, a tensile intrinsic stress appears in the film when it is cooled from the curing temperature ($\geq 300^\circ\text{C}$). Furthermore, the chemical reaction (imidization) and evaporation of solvent/photosensitive groups of the polymer cause a loss of volume, thereby adding to the intrinsic tensile stress. Substrate curvature experiments have been performed on 3-inch, 380- μm -thick silicon wafers, which were covered with a 1.5- μm -thick thermal silicon dioxide layer. A layer of the photosensitive polyimide precursor HTR3-200 from OCG Microelectronics was spun onto the wafer (3000 rpm, 20 s) and cured at 300°C for 1 h in a conventional convection oven. Before applying the precursor, a silane adhesion promoter, γ -APS (aminopropyltriethoxysilane), was used to treat the silicon oxide surface. The average stress measured in the films was 33 MPa, which is in good agreement with previously published values ranging from 30 MPa to 70 MPa. Furthermore, the stress was monitored over a period of 80 days (Fig. 2) to determine the occurrence of relaxation phenomena. As can be seen from the figure, the stress in the film decreases over time. However, no exact information about the relaxation can be obtained, since the strain induced by the substrate also decreases as the deflection decreases. The results suggest that the stress of the polyimide tends to level off around a value of approximately 20 MPa. This is further supported by the measurements shown in Fig. 3, which were performed on a similar polyimide film cured at 300°C for 1 h in a vacuum oven with 2 mbar N_2 applied. These data indicate that the stress relaxes quickly (within a few days) and remains stable at a specific level, which in this case was approximately 23 MPa.

The dynamic mechanical properties of the viscoelastic polyimide were investigated by Pecht and Wu.⁽¹⁶⁾ As expected for polymers, Young's modulus was found to depend on the strain, temperature and strain rate. Also, creep strain of the polyimide depends on the temperature and the stress level. However, since the glass transition temperature of polyimides is at least as high as the curing temperature ($\geq 300^\circ\text{C}$),⁽¹⁴⁾ these effects are

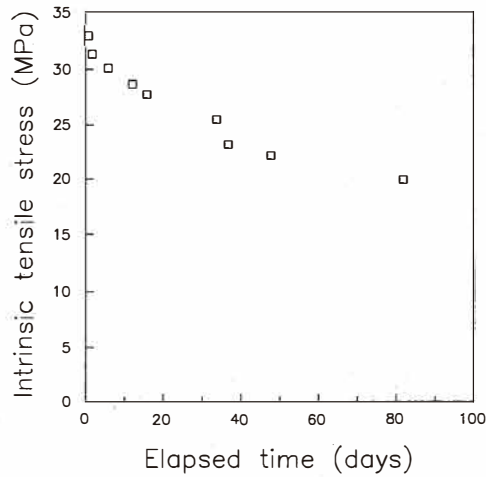


Fig. 2. Measured stress of a HTR3 polyimide film cured in a convection oven vs elapsed time.

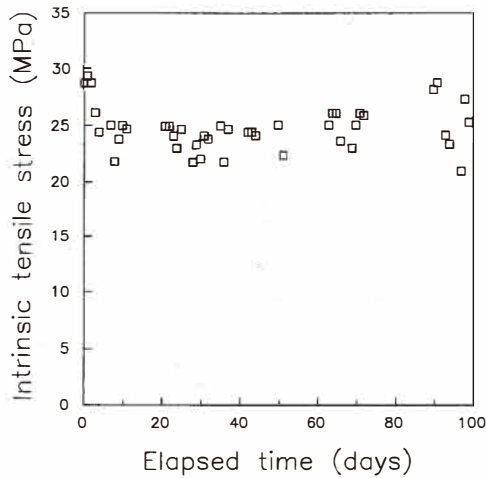


Fig. 3. Measured stress of HTR3 polyimide film cured in 2 mbar N₂ vs elapsed time.

expected to have little influence on the device operations at room temperature, because the effects are very slow (taking several days). Therefore, only the issue of long-term stability regarding the intrinsic stress (Figs. 2 and 3) must be considered. This issue is best treated by keeping it in mind when evaluating the actual sensor devices, since these complex relaxation mechanisms will eventually depend on the complete structure containing the

polyimide film(s).

The properties of polyimide are summarized in Table 1; for the purpose of comparison, values for silicon and silicon nitride are also given. Comparing the intrinsic stress and Young's modulus of the polyimide, it is clear that any micromechanical polyimide structure will be influenced by the stress. This means that the mechanical sensitivity of such structures will not be higher than that for silicon nitride structures. However, since the density of the polyimide is very low, large structures may be fabricated without the problem of resonances arising, thereby increasing the mechanical sensitivity. From these results it is concluded that the use of polyimide in mechanical sensors may be feasible if the properties can be controlled. Furthermore, new (photosensitive) polyimides with thermal expansion properties closely matched to silicon are being developed,⁽¹⁷⁾ and therefore it is believed that polyimide layers with lower stress levels and higher mechanical sensitivities than currently possible can be produced in the future.

3. Applications in Capacitive Sensors

For the fabrication of capacitive mechanical sensors in polyimide, a complete process module has been developed.⁽¹⁸⁾ Using this process, different sensors may be fabricated simply by modifying the masks in the process, similar to IC technology. The fabrication process, involving both surface and bulk micromachining, has been described in detail elsewhere^(19,20) and will therefore only be briefly discussed here.

The process is carried out on silicon substrates covered with an insulating layer, such as thermal silicon oxide. In the event that the process is performed on substrates already containing integrated electronic circuitry, this layer will be present from the IC process. First, a Cr/Au/Cr electrode layer is deposited and patterned using lift-off with photoresist, and the first PI layer is spun on, patterned and cured (Fig. 4(a)). All polyimide layers described in the following were produced using the HTR3-200 photosensitive polyimide

Table 1
Properties of polyimide, silicon and silicon nitride.

	Polyimide	Silicon (110)	Silicon nitride
Dielectric constant	3.1–3.5	11.7–12	7–10
Dissipation factor ($\tan \delta$)	10^{-3}	—	—
Breakdown electrical field	1.6–3.3 MV/cm	0.1 MV/cm	1–10 MV/cm
Resistivity	$10^{16} \Omega\text{cm}$	0.1–60 Ωcm	$10^{12} \Omega\text{cm}$
CTE	50 ppm/°C	3 ppm/°C	2.5–3 ppm/°C
Density	1,430 kg/m ³	2,329 kg/m ³	3,400 kg/m ³
Intrinsic stress	20–70 MPa	0	–50–100 MPa
Young's modulus	4–10 GPa	170 GPa	130 GPa
Poisson's ratio	0.45	0.066	0.2

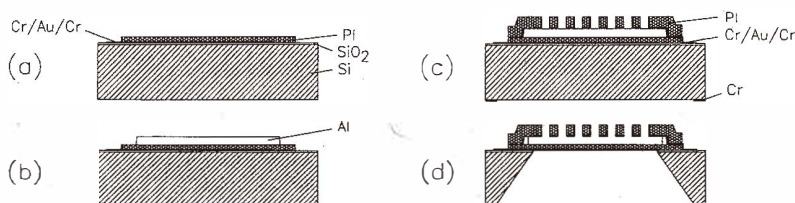


Fig. 4. Polyimide sensor process. (a) Deposition of the first Cr/Au/Cr metal electrode and polyimide layer. (b) Deposition of the Al sacrificial layer. (c) Deposition of the second Cr/Au/Cr metal electrode and polyimide layer, and deposition of the Cr etch mask on the back of the Si substrate. (d) Etching of the Al sacrificial layer and Si substrate.

precursor from OCG Microelectronics Inc., in which different layer thicknesses were realized by changing the spinning parameters and/or the viscosity of the precursor by adding solvent. After curing, the Al sacrificial layer is deposited and patterned (Fig. 4(b)), and the second Cr/Au/Cr electrode and polyimide layers are applied in a similar manner to the first layers. Subsequently, a Cr layer is deposited on the back of the substrate to serve as a mask for the etching of the silicon substrate (Fig. 4(c)). Finally, the sacrificial layer is etched in a chemical solution containing phosphoric acid, and the silicon substrate is etched using dry reactive ion etching (RIE) with a gas composition of $\text{SF}_6/\text{CHF}_3/\text{O}_2$ (Fig. 4(d)). During the etching of the silicon substrate, the first Cr/Au/Cr electrode layer acts as an etchstop. The device shown in Fig. 4(d) has two metallic polyimide diaphragms, and was developed for use as a condenser microphone, which is one of the three possible capacitive sensor applications described in the following.

3.1 Polyimide condenser microphone

The desire to develop a condenser microphone with an integrated signal detection circuit has been the impetus for the evolution of capacitive sensors in polyimide. As for all capacitive sensors, the advantages of integrating a condenser microphone with the detection circuit is that the parasitic loading of the sensor can be minimized, together with a reduction of the induced noise. This improvement in the performance of the microphone is believed to make the micromachined devices competitive with the conventional technology of electret microphones for applications such as hearing aids. The use of condenser microphones, which are biased by an external DC voltage, may be favorable compared to electret microphones, since the issue of charge stability on the electret can be eliminated. Furthermore, the introduction of micromachining has made it possible to realize structures with air gaps between the diaphragm and backplate on the order of a few microns, compared with $> 10 \mu\text{m}$ for conventional technologies. This has resulted in a significant reduction in the required DC bias voltage from $> 200 \text{ V}$ to $5\text{--}20 \text{ V}$, which may be generated from a small battery with a DC-DC voltage converter circuit (a charge pump).

In Figs. 5 and 6, the cross-sectional view and SEM micrograph of a polyimide condenser microphone are shown. The condenser microphone is, in principle, a pressure sensor sensitive to pressure variations down to ten orders of magnitude smaller than normal ambient pressures. The microphone basically consists of a diaphragm and a backplate, separated by an air gap. As the diaphragm moves according to the sound pressure variations, the acoustic holes in the backplate allow the air in the air gap to flow freely to and from the gap.⁽¹⁹⁾ The number of holes in the backplate is related to the height of the air gap, and must be large enough to minimize the viscous damping of the air flow, thereby ensuring a sufficiently high cut-off frequency of the microphone. The movement of the diaphragm, which results in a changing capacitance between the diaphragm and backplate, is normally detected by applying a static electrical field in the air gap and measuring the small variations of electrical potential over the microphone using an amplifier with very high input impedance.

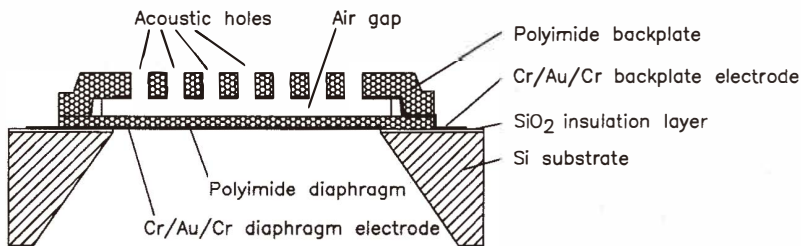


Fig. 5. Cross-sectional view of the polyimide condenser microphone.

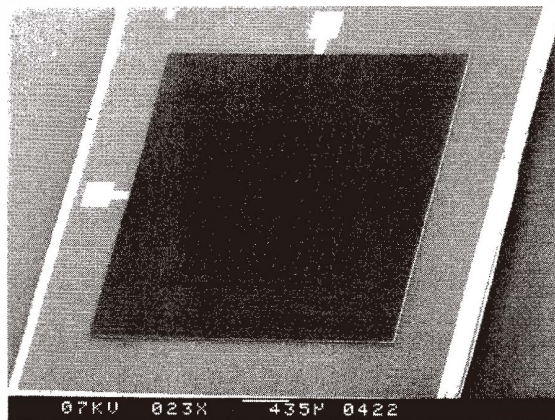


Fig. 6. SEM micrograph of the front of the polyimide condenser microphone.

The microphone was fabricated according to the process described above, in which the thicknesses of the diaphragm and the perforated backplate were $0.9\ \mu\text{m}$ and $18\ \mu\text{m}$, respectively. The air gap was $1.5\ \mu\text{m}$, and devices with diaphragm sizes of $1.6\ \text{mm}$ (A) and $2.1\ \text{mm}$ (B) were realized. The microphones were tested in an acoustical measurement setup, in which the frequency response and sensitivity could be obtained by comparison to that of a known Brüel and Kjær reference microphone.⁽²¹⁾ The measured open-circuit sensitivity as a function of the DC bias voltage and the frequency response of the two sizes of microphones are shown in Figs. 7 and 8. The measurements of the sensitivity vs DC bias voltage (Fig. 7) demonstrate the well-known properties of stability of the condenser microphone. The characteristic curves containing a linear, exponential, and over-exponential segment illustrate the influence of the electrostatic attraction forces between the diaphragm and the backplate caused by the DC bias voltage. Above a certain level known as the critical bias voltage (CBV), these forces cause a collapse of the structure. The CBV for the microphones was measured to be $23\ \text{V}$ for (A) and $21\ \text{V}$ for (B), and the values, together with the shape of the curves, were found to be in good agreement with the results of theoretical analyses.⁽¹⁹⁾ The frequency responses of the microphones (Fig. 8), operated at a bias voltage of $15\ \text{V}$, were found to be flat ($\pm 2\ \text{dB}$) in the measured range between $100\ \text{Hz}$ and $15\ \text{kHz}$. Furthermore, open-circuit sensitivities of $5.1\ \text{mV/Pa}$ (A) and $8.1\ \text{mV/Pa}$ (B) were measured at $1\ \text{kHz}$, and the noise levels were determined to be $28\ \text{dB(A) SPL}$ (A) and $24\ \text{dB(A) SPL}$ (B).

3.2 Polyimide pressure sensor

The polyimide process technology can also be directly exploited to fabricate a capacitive pressure sensor (Fig. 9). This structure can be realized by modifying the masks, whereby an opening is added in the first Cr/Au/Cr- and polyimide layers and the holes in the second polyimide layer are removed. In this situation, what was previously the thick polyimide backplate in the microphone now acts as the sensing diaphragm in the pressure sensor. The opening in the silicon substrate is reduced such that the first polyimide layer acts as electrical insulation.

From theoretical considerations, in terms of the deflection of the polyimide diaphragm, a sensor for a pressure range of $1\ \text{bar}$ has been designed and fabricated.⁽²⁰⁾ The SEM micrograph in Fig. 10 depicts the front of the device and shows the polyimide diaphragm and the electrical connections. The size and thickness of the diaphragm were chosen to be $700 \times 700\ \mu\text{m}$ and $15\ \mu\text{m}$, the height of the air gap was $5\ \mu\text{m}$ and the thickness of the first polyimide insulation layer was $0.5\ \mu\text{m}$. These dimensions yield a theoretical center deflection of $3.6\ \mu\text{m}$ of the diaphragm for a pressure of $1\ \text{bar}$, and a sensor capacitance of $0.62\ \text{pF}$ with no pressure applied. The theoretical relationship between the sensor capacitance and the applied pressure difference is shown in Fig. 11. As can be seen, a relative change of $0.14\ \text{pF}$ (22%) of the capacitance is expected in the range of $0-1\ \text{bar}$.

The sensor chip was mounted on a printed circuit board and tested in a setup where the pressure could be applied to the back of the device. The capacitance of the sensor was monitored using an HP 4194A impedance analyzer, and the resulting measurements are shown in Fig. 12. It appears that the measurements are somewhat different from the theoretical results, since the relative change $\Delta C/C$ is only 3.2% . This can be explained by

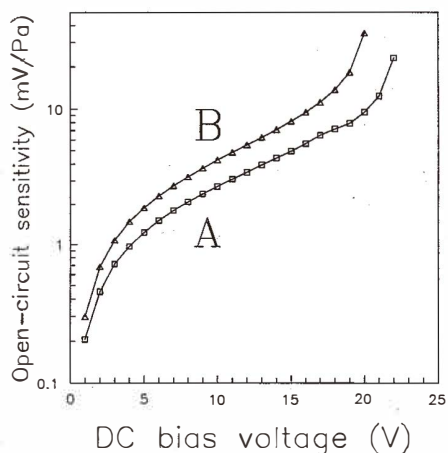


Fig. 7. Measured open-circuit sensitivity vs DC bias voltage (frequency: 1 kHz) of the polyimide condenser microphones (A: 1.6 mm, B: 2.1 mm).

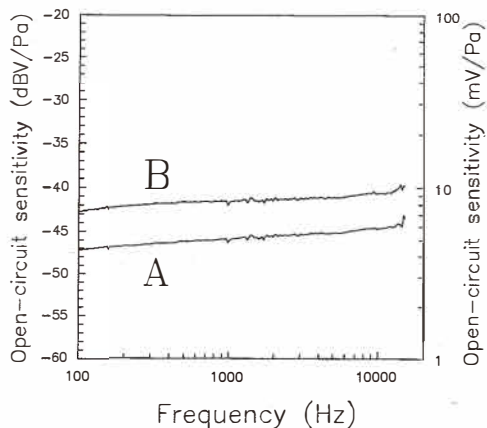


Fig. 8. Measured frequency response (DC bias voltage: 15 V) of the polyimide condenser microphones (A: 1.6 mm, B: 2.1 mm).

the parasitic capacitance of the connections between the sensor and the analyzer, which also causes the high value of the measured sensor capacitance. Subtracting a parallel parasitic capacitance of 2.7 pF from the measurements yields a relative change $\Delta C/C$ of 17%, which is in good agreement with the results of the theory. This is a good illustration of the importance of the minimization of the parasitic effects in capacitive sensors.

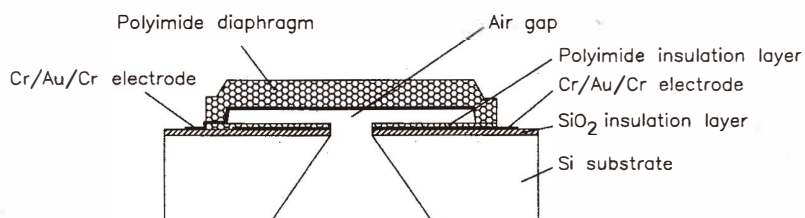


Fig. 9. Cross-sectional view of the polyimide pressure sensor.

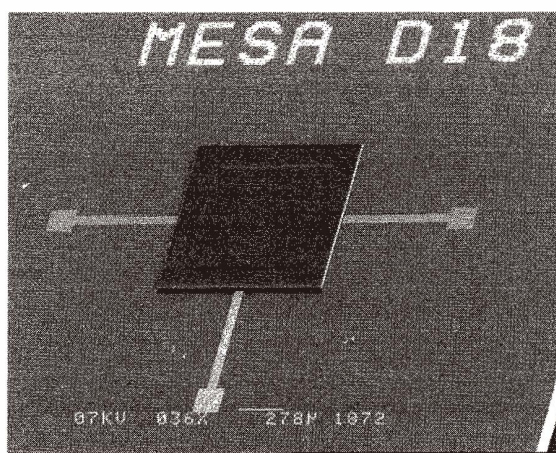


Fig. 10. SEM micrograph of the front of the polyimide pressure sensor.

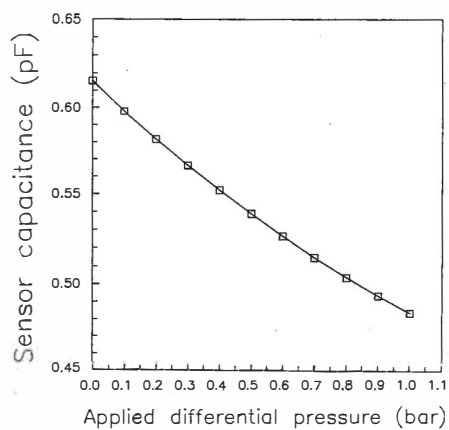


Fig. 11. Calculated capacitance of the pressure sensor vs applied differential pressure.

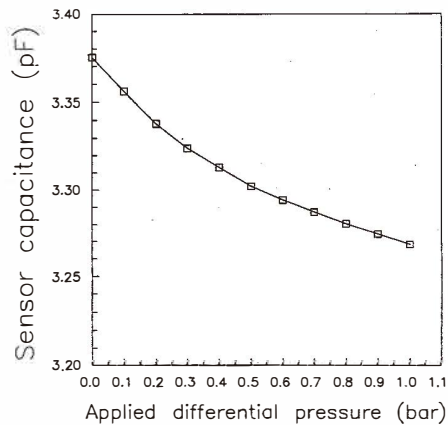


Fig. 12. Measured capacitance of the pressure sensor vs applied differential pressure.

3.3 Polyimide uniaxial accelerometer

A third possibility of the fabrication process is the fabrication of a capacitive accelerometer (Figs. 13 and 14). Since the viscoelastic polymer material can absorb much larger energies than solids at high strain rates (shocks) without breakage, this accelerometer could be useful in applications that require resistance to very large shocks. The fabrication of this device is simpler than those of the condenser microphone and pressure sensor, since no etching of the silicon substrate is required in this purely surface-micromachined structure. As for the pressure sensor, the first Cr/Au/Cr- and polyimide layers serve, respectively, as a fixed counterelectrode and electrical insulation layer. The device consists of a seismic mass in the form of a polyimide plate suspended diagonally on four polyimide beams, all of which are realized in the second Cr/Au/Cr- and polyimide layers.

In operation, an external force exerted on the free structure will cause it to deflect, and since the beam suspension is much more compliant than the plate (mass) itself, it can be assumed that the plate will experience a piston-type movement. The dynamic mechanical behavior can be described by the linear circuit shown in Fig. 15. In this equivalent mechanical circuit, the source F represents the force applied to the seismic mass, the coil M is the inertia of the seismic mass, the capacitor C is the compliance of the four beam suspensions, and the resistor R is the damping caused by air flowing in the thin air gap between the seismic mass and the substrate. The values of the components for the structure shown in Fig. 13 are given by

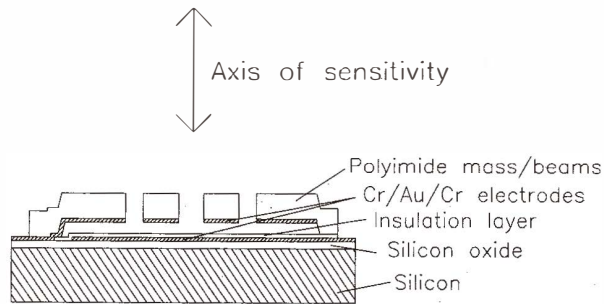


Fig. 13. Cross-sectional view of the polyimide accelerometer.

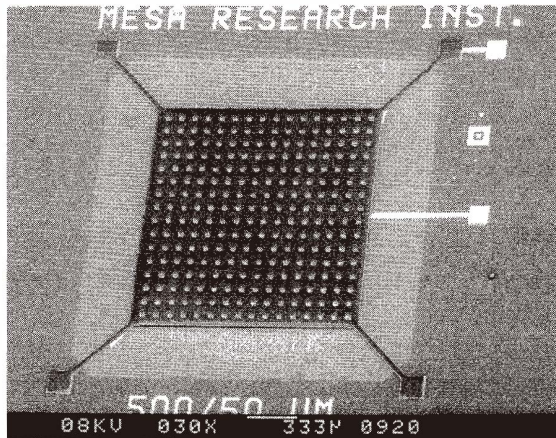


Fig. 14. SEM photograph of the front of the polyimide accelerometer.

$$M = \left(1 - \frac{4a^2}{b^2}\right) L^2 (h\rho + h_e\rho_e) \quad F = Ma \tag{1}$$

$$C = \left(\frac{4EW_{\text{beams}}h^3}{L_{\text{beams}}^3} + \frac{4\sigma W_{\text{beams}}h}{L_{\text{beams}}} \right)^{-1} \quad R = \frac{1.22\eta\pi L^2 b^2}{h_a^3} B,$$

where $2a$ and b are the size and center-to-center distance of the holes in the plate, L and h are the size and the thickness of the polyimide plate and beams, ρ and E are the density and Young's modulus of polyimide, h_e and ρ_e are the thickness and the density of the second Cr/

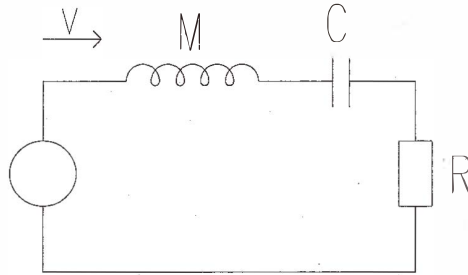


Fig. 15. Mechanical equivalent circuit of the accelerometer.

Au/Cr layer, σ is the intrinsic stress, W_{beams} and L_{beams} are the width and length of the polyimide beams, h is the dynamic viscosity of air ($17.1 \mu\text{Pa s}$), h_a is the height of the air gap, and B is a value related to the position and size of the holes in the polyimide plate:⁽²²⁾

$$B = \frac{1}{4} \ln \left(\frac{X_0^2}{R_h^2} \right) - \frac{3}{8} + \frac{1}{2} \frac{R_h^2}{X_0^2} - \frac{1}{8} \frac{R_h^4}{X_0^4} \quad (2)$$

$$X_0 = 0.565b \quad R_h = a\sqrt{2}.$$

The flow (current) v in the equivalent circuit denotes the velocity of the seismic mass, and under the harmonic condition, the amplitude of the movement may be derived simply by dividing the velocity by the angular frequency ω . An accelerometer with the following dimensions was designed and fabricated: L 2 mm; h 13 μm ; $2a$ 40 μm ; b 80 μm ; h_a 2 μm ; W_{beams} 50 μm ; L_{beams} 500 μm . A calculation of the equivalent circuit yields a mechanical sensitivity of 6.47 nm/g, corresponding to a nominal sensitivity $\Delta C/C$ of 0.32%/g. The accelerometer was mounted on a mechanical shaker and tested using an amplitude-modulated (AM) detection circuit, as shown in Fig. 16. The AM circuit is an alternative to the DC biasing used for the condenser microphone, and allows measurements of static accelerations. A 200 kHz AC source with an amplitude of 2.1 V_{pp} was applied to the charge amplifier with the accelerometer C_{sens} and the feedback capacitor C_{fb} , and the bias resistor R_{b} was used to prevent charging of the input. The 200 kHz carrier signal was then removed with the low-pass filter R_{lp} and C_{lp} , leaving an output signal v_{out} which was directly proportional to the change of the sensor capacitance.

The applied acceleration was measured using a reference accelerometer, and the recorded change of capacitance $\Delta C/C$ vs the acceleration is shown in Fig. 17 for a frequency of 100 Hz. As can be seen, the measured sensitivity (0.43%/g) is somewhat higher than the predicted value; however, the linearity in the measured range is still good. This implies that the compliance is higher in the realized devices. The frequency response

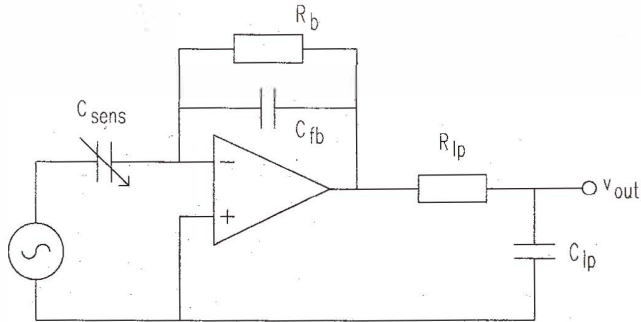


Fig. 16. AM detection circuit for the accelerometer.

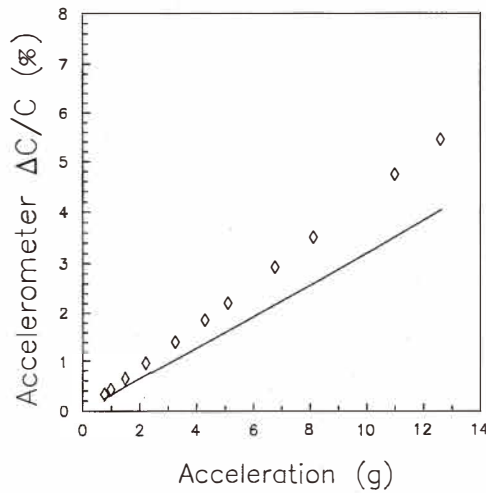


Fig. 17. Change of capacitance vs applied acceleration (Line: theory; \diamond : measurement) of the accelerometer.

of the accelerometer was measured in a range between 20 Hz and 3 kHz. In Fig. 18, the measured nominal sensitivity is shown together with the simulated response derived from eqs. (1) and (2). For frequencies below 1 kHz, there is reasonable agreement between the measurements and the theory. The resonance peaks at higher frequencies are not caused by the sensor itself, but rather from insufficiently firm attachment of the sensor onto the shaker.

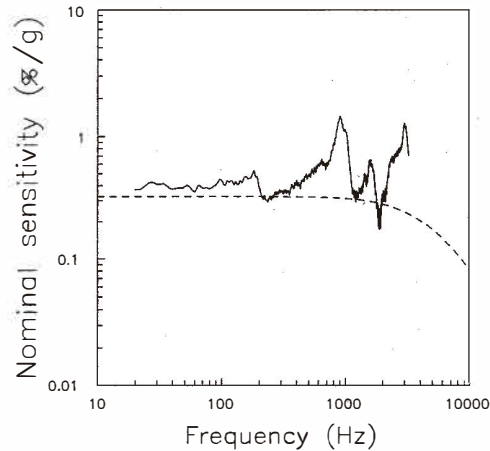


Fig. 18. Frequency response of the accelerometer (Dashed line: theory; solid line: measurement).

4. Conclusions and Discussions

In this paper, the process technology and material properties of polyimide have been reviewed, and a modular fabrication process for capacitive mechanical sensors has been suggested. The process was developed with the intention of achieving full integration of the sensor and the electronic signal conditioning circuitry in a simple and reliable manner, to fully exploit the high performance of capacitive sensors. The best solution to this complex problem is to develop a sensor process that can be performed independently of any IC process, thereby providing the best flexibility of the complete fabrication. The use of polymers in the sensor makes it possible to realize a fabrication process that is fully IC-compatible. One of the best-suited polymers appears to be polyimide, since it is mechanically and chemically very stable and yet can be fabricated in a simple manner by spin coating and baking. Introduction of this material has resulted in a low-temperature (< 300°C) sensor fabrication process, which can be performed as a postprocess directly on substrates containing integrated circuits.

Polyimide is a well-characterized material, since it is used in IC processes and hybrid packaging as an electrical insulation layer. Therefore, a large variety of polyimide precursors are commercially available both with and without photosensitive properties. The structures described in this paper have all been made from one type of photosensitive polyimide (HTR3 from OCG Microelectronics), which can be applied in layers from < 1 μm to > 50 μm thick. The three sensor applications illustrated in this paper serve to demonstrate how different device structures can be realized without changing the fabrication process, which adds to the flexibility of the process. Based on the results of the implemented sensor structures, it may be concluded that capacitive sensors with excellent

properties can be produced using this process. There are, however, issues regarding long-term stability of polymers and the structures based on them that must be considered. For polyimide, no long-term chemical degradation is known to take place; however, as indicated from the measurements in this study some relaxation of the intrinsic stress in the polyimide can be expected. Measurements on two-year-old microphones show no detectable change of sensitivity, which suggests that relaxation, if any, takes place shortly after fabrication. Unfortunately, it is well known that polyimide absorbs water, leading to a change in the dielectric constant by up to 35% over the full humidity range.⁽⁹⁾ This may seem a significant change; however, for the structures outlined in this paper, only a thin film of polyimide is electrically involved in the sensor and it is always in series with the air gap. Therefore, since the sensor capacitance is largely determined by the air gap, calculations show that the influence of humidity will be < 0.5 dB for the microphone and < 1% for the pressure sensor and the accelerometer, which in practice would be negligible. A more significant parameter is the thermal expansion, which, for conventional polyimides, is ≈ 16 times larger than silicon. For increasing temperatures, this leads to a reduction in the intrinsic stress in the polyimide film, causing an increase in the mechanical sensitivity of the structures. Recent developments in polymer science seem to provide a solution to this problem through the fabrication of new polyimide materials with thermal properties matching those of silicon.^(17,23) With the emergence of such new materials, polymer processing may become a dominating fabrication method for smart sensors in the future, due to its simplicity and IC-compatibility.

Acknowledgements

The authors are indebted to Johan Bomer for the fabrication of the devices, Bert Otter for providing the SEM micrographs, and to the Dutch Technical Foundation (STW) for financial support.

References

- 1 K. Petersen: Proc. IEEE **70** (1982) 420.
- 2 S. Middelhoek and A. C. Hoogerwerf: Sensors and Actuators **8** (1985) 39.
- 3 W. Kuehnel and S. Sherman: Sensors and Actuators A **45** (1994) 7.
- 4 S. M. Sze: Semiconductor Devices, Physics and Technology (Wiley, New York, 1985) p. 367.
- 5 S. Fang and J. P. McVittie: IEEE Electron Dev. Lett. **13** (1992) 288.
- 6 Y. K. Lee and J. D. Craig: ACS Symposium series **184** (1982) 107.
- 7 D. S. Soane: Polymers in Microelectronics: Fundamentals and Applications (Elsevier, Amsterdam, 1989).
- 8 N. J. Chou, D. W. Dong, J. Kim and A. C. Liu: J. Electrochem. Soc. **131** (1984) 2335.
- 9 R. J. Jensen, J. P. Cummings and H. Vora: IEEE Trans. Comp. Hyb. Manufact. Technol. **CHMT-7** (1984) 384.
- 10 D. L. Pappas, J. J. Cuomo and K. G. Sachdev: J. Vac. Sci. Tech. A **9** (1991) 2704.
- 11 P. G. Rickerl, J. G. Stephanie and P. Slota: IEEE Trans. Comp. Hyb. Manufact. Technol. **CHMT-12** (1987) 690.
- 12 A. M. Wilson: Thin Solid Films **83** (1981) 145.

- 13 L. B Rothman: *J. Electrochem. Soc.* **127** (1980) 2216.
- 14 C. Goldsmith, P. Geldermans, F. Bedetti and G. A. Walker: *J. Vac. Soc. Tech. A* **1** (1983) 407.
- 15 M. Mehregany, R. T. Howe and S. D. Senturia: *J. App. Phys.* **62** (1987) 3579.
- 16 M. Pecht and X. Wu: *IEEE Trans. Comp. Hyb. Manufact. Technol. B* **17** (1994) 632.
- 17 O. Rohde, P. Smolka, P. A. Falcigno and J. Pfeifer: *Polymer Eng. Sci.* **32** (1992) 1623.
- 18 Patent application no. 1001733, Rijswijk, the Netherlands, November, 1995.
- 19 M. Pedersen, W. Olthuis and P. Bergveld: Accepted for publication in *Sensors and Actuators A*.
- 20 M. Pedersen, M. G. H. Meijerink, W. Olthuis and P. Bergveld: Accepted for publication in *Sensors and Actuators A*.
- 21 M. Pedersen, R. Schellin, W. Olthuis and P. Bergveld: *J. Acoust. Soc. Am* **101** (1997) 2122.
- 22 Z. Skvor: *Acustica* **19** (1967/68) 295.
- 23 A. E. Nader, K. Imai, J. Craig, C. N. Lazaridis, D. O. Murray III, M. T. Pottiger, S. A. Dombchik and W. J. Lautenberger: *Polymer Eng. Sci.* **32** (1992) 1613.